



UNIVERSITY OF LEEDS

This is a repository copy of *Ubiquitous Presence of Fe(II) in Aquatic Colloids and Its Association with Organic Carbon*.

White Rose Research Online URL for this paper:  
<http://eprints.whiterose.ac.uk/127225/>

Version: Accepted Version

---

**Article:**

von der Heyden, BP, Hauser, EJ, Mishra, B et al. (6 more authors) (2014) Ubiquitous Presence of Fe(II) in Aquatic Colloids and Its Association with Organic Carbon. *Environmental Science & Technology Letters*, 1 (10). pp. 387-392. ISSN 2328-8930

<https://doi.org/10.1021/ez500164v>

---

(c) 2014 American Chemical Society. This is an author produced version of a letter published in *Environmental Science & Technology Letters*. Uploaded in accordance with the publisher's self-archiving policy.

**Reuse**

Items deposited in White Rose Research Online are protected by copyright, with all rights reserved unless indicated otherwise. They may be downloaded and/or printed for private study, or other acts as permitted by national copyright laws. The publisher or other rights holders may allow further reproduction and re-use of the full text version. This is indicated by the licence information on the White Rose Research Online record for the item.

**Takedown**

If you consider content in White Rose Research Online to be in breach of UK law, please notify us by emailing [eprints@whiterose.ac.uk](mailto:eprints@whiterose.ac.uk) including the URL of the record and the reason for the withdrawal request.



[eprints@whiterose.ac.uk](mailto:eprints@whiterose.ac.uk)  
<https://eprints.whiterose.ac.uk/>

# Ubiquitous presence of Fe(II) in aquatic colloids and its association with organic carbon

Bjorn P. von der Heyden<sup>1\*</sup>, Emily J. Hauser<sup>2</sup>, Bhoopesh Mishra<sup>3</sup>, Gustavo A. Martinez<sup>4</sup>, Andrew R. Bowie<sup>5,6</sup>, Tolek Tyliczszak<sup>7</sup>, Thato N. Mtshali<sup>8</sup>, Alakendra N. Roychoudhury<sup>1</sup>, Satish C. B. Myneni<sup>2</sup>

1. Department of Earth Sciences, Stellenbosch University, Private Bag X1, Matieland, 7602, South Africa
2. Department of Geosciences, Princeton University, Princeton, NJ 08544, USA
3. Physics Department, Illinois Institute of Technology, Chicago, IL 60616, USA
4. Crops and Agroenvironmental Department, College of Agricultural Sciences, University of Puerto Rico, Mayagüez, Puerto Rico
5. Antarctic Climate and Ecosystems CRC, Private Bag 80, Hobart, Tasmania 7001, Australia
6. Institute of Marine and Antarctic Studies, University of Tasmania, Private Bag 129, Hobart, Tasmania 7001, Australia
7. Advanced Light Source, Lawrence Berkeley National Laboratory, University of California, Berkeley, CA 94720, USA
8. Council for Scientific and Industrial Research, P.O. Box 320, Stellenbosch, 7600, South Africa

**\*Corresponding Author:**

bjorn.vonderheyden@exxaro.com

Phone: (+27) 84 685 2642

## ABSTRACT

Despite being thermodynamically less stable, small ferrous colloids (60 nm to 3 µm in diameter) remain an important component of the biogeochemical cycle at Earth's surface, yet their composition and structure, and the reasons for their persistence are still poorly understood. Here we use X-ray based Fe L-edge and carbon K-edge spectromicroscopy to address the speciation and organic-mineral associations of ferrous, ferric and Fe-poor particles collected from sampling sites in both marine and fresh water environments. We show that Fe(II) rich phases are prevalent throughout the different aquatic regimes yet they exhibit a high degree of chemical heterogeneity. Furthermore, we show that Fe-rich particles show strong associations with organic carbon, specifically for the association of Fe(II) particles with carboxamide functional groups, suggesting a microbial role in the preservation of Fe(II). These findings have significant implications for the behaviour of Fe(II) colloids in oxygenated waters, and their role in different aquatic biogeochemical processes.

## INTRODUCTION

Iron minerals are common in soils and sediments, where they represent important sources of Fe for biological processes and, because of their large and highly reactive surface area, they act as strong sorbents for various contaminants and nutrients<sup>1,2</sup>. In aquatic environments, Fe species can persist as colloids in the micron to submicron size range, where their stability is governed by water composition and mineral surface chemistry. Photochemical transformations, mineral dissolution, and changes to the Fe redox state can further modify the fates of these phases and their associated contaminants and nutrients<sup>3-5</sup>. While the importance of colloidal Fe in various biogeochemical processes is well understood, little attention has been paid to the speciation, stability and mineralogical associations of Fe phases in the colloidal fraction of oxygenated natural waters.

With the advent of synchrotron based X-ray spectromicroscopy methods, the structures of Fe colloids, their chemical and mineralogical characteristics as well as the factors affecting Fe colloid stability can now be probed directly<sup>6,7</sup>. Several researchers have examined the chemistry of natural Fe-containing particles in the particulate fraction using X-ray imaging and speciation techniques at both the K-, and L-edges of Fe<sup>8-15</sup>. The X-ray spectromicroscopy at the Fe K-absorption edge, which is highly sensitive to Fe concentration and has lower spatial resolution (>100-150 nm to a few microns), has been utilized to determine the average Fe speciation in heterogeneous samples<sup>12,16</sup> and to determine particle specific speciation in larger micron-sized particulates<sup>14</sup>. In comparison, spectromicroscopy at the Fe L-absorption edge has a much higher spatial resolution (down to a few nanometers) and has successfully been applied to study Fe-biomineralization<sup>10,11</sup> and the speciation of Fe-colloids from hydrothermal vents<sup>13</sup> and the open ocean<sup>15</sup>.

In this study we applied Fe L-edge and C K-edge scanning transmission X-ray microscopy (STXM) to identify the common forms of Fe in the colloidal fractions of natural waters and the association of different Fe pools with natural organic moieties. This zone-plate based X-ray spectromicroscopy is ideal for the study of aquatic colloids as samples can be examined in their native hydrated state, down to a spatial resolution of 10-15 nm and without any special sample preparation. Furthermore, the Fe L-edge is characterised by a high absorption cross-section (which results in high contrast images) and X-ray Absorption Near-edge Structure (XANES) spectra that are rich in chemical and structural information<sup>15,17,18</sup>. Von der Heyden and co-workers<sup>15</sup> showed the identification of some of the Fe mineral phases using the energy difference between the two L<sub>3</sub> peaks ( $\Delta E_V$  value) and the quotient of their peak intensities, given as the intensity ratio value (Fig. 1). Because each individual Fe mineral has a unique Fe coordination environment, and thus XANES spectral shape, Fe mineral phases can be characterised by a unique combination of  $\Delta E_V$  and intensity ratio values (Fig. 2). Here we exploit

the information contained in these L<sub>3</sub>-edge spectral parameters to evaluate the speciation of Fe in colloids collected from both marine and fresh waters, and show the ubiquitous presence of thermodynamically unstable Fe(II) in association with carbon moieties.

## MATERIALS AND METHODS

Lacustrine samples were collected from fresh water systems in New Jersey and Puerto Rico and the marine samples focused primarily on the Southern Ocean and the western South Pacific Ocean. To attain a sufficient number of particles for STXM analysis, a range of site-specific sampling techniques was employed and detailed descriptions are documented in the supporting information (SI 1). Ocean water samples, typically characterised by a low suspended particle load, required pre-concentration procedures using either McLane pumps or vacuum filtration whereas freshwater samples, with high particle loads, could be collected without the need for prior filtration. In all instances, trace-metal clean techniques were followed and, because of sensitivity to contamination, marine water samples were collected following the rigorous guidelines set out in the GEOTRACES protocol<sup>19</sup>.

All Fe L-edge and C K-edge spectromicroscopic analyses were conducted at the Molecular Environmental Sciences end-station at the Advanced Light Source<sup>8</sup>. Samples were prepared on silicon nitride (SiN<sub>3</sub>) membrane windows according to the procedures outlined in the supporting information (SI 2). During STXM experimentation, Fe-rich particles were located on the SiN<sub>3</sub> sample window using coarse 10x10 μm<sup>2</sup> or 30x30 μm<sup>2</sup> image maps generated by subtracting an edge-region (709-710 eV) X-ray image from an image of the same area collected at an energy below the Fe L<sub>3</sub> absorption edge (700 eV). Once located, Fe-rich regions were analysed for their XANES spectra using either linescans or image stacks (10-50 nm spatial resolution) over the Fe L<sub>2,3</sub> edge region. Energy increments of 0.5 eV were used above and below the edge (695-703 eV; 715-730 eV) and a step-size of 0.2 eV was used close to the Fe L<sub>3</sub> edge (703-715 eV).

Once Fe-enriched particles had been identified and analysed, the corresponding regions on SiN<sub>3</sub> window were evaluated at the carbon K-edge for the prevalence of organic phases (Fig. 1) by applying the procedures described above. XANES spectra were collected for both Fe-enriched and Fe-poor organic particulates by generating either line-scans or image stacks; using energy increments of 0.2 eV at the C K-edge edge (283-300 eV) and 0.5 eV above and below the edge (280-283 eV; 300-315 eV). All collected C K-edge spectra were calibrated using the characteristic absorption feature at 284.8 eV.

Although this study focused on the Fe L-edge and C K-edge, we also strengthened our data set with complementary nitrogen K-edge and Fe K-edge XANES data. For identified Fe enriched particles, XANES analyses were conducted at the N K-edge region (385-420 eV) following the analysis protocols

described for the Fe L-edge and the C K-edge. The collected N K-edge XANES spectra for Fe enriched particles however, typically exhibited weak signals due to low N abundances. Because of larger sample volumes, bulk Fe K-edge analyses could be conducted on the sediment trap samples collected from Lake La Plata, Puerto Rico. Analyses were conducted at the X-18B beamline, National Synchrotron Light Source (Brookhaven National Laboratories, NY) and the analysis protocol and beamline specifications are described in the supporting information (SI 3).

## RESULTS AND DISCUSSION

The collection of high quality microscopic and spectroscopic data for small colloids on a particle-by-particle basis is a time consuming process. The presented dataset represents a significant investment (over 20 days) in synchrotron beam-time, as each SiN<sub>3</sub> sample window requires 1-3 days for complete characterisation (at both Fe- and C- absorption edges). Fe(III) particles commonly occurred as the smaller sized colloids (down to 20 nm diameter) whereas Fe(II)-rich particles were typically larger (0.06 - 2.6 μm) and were observed in all of the sampling sites considered in this study. In the open-ocean domain Fe can be a limiting nutrient and consequently and despite our particle-concentrating sampling protocol, Fe-enriched particles were sparse and difficult to locate (e.g. only 3-10 particles or aggregates per SiN<sub>3</sub> window for some marine samples). Open-ocean Fe-rich particles, and particle aggregates were typically quasi-spherical in shape and tended towards smallest size domains (20 nm to ~ 800 nm), with some larger particles collected at depth. In stark contrast, SiN<sub>3</sub> sample plates prepared using freshwater samples were highly enriched in Fe, with much of the Fe associated with organic flocs and mineral aggregates of up to several microns in diameter.

### Speciation of Iron

#### *Southern Ocean samples*

Iron-rich particles in the South Atlantic and Southern Oceans have previously been shown to classify into five distinctly different chemical categories according to their ΔeV and intensity ratio spectral parameters<sup>15</sup>. Despite the oxic nature of surface seawater, a remarkable 12% of particles analyzed in this study were classed as either purely ferrous, or as Fe(II)-rich mixed valence phases. The majority of these particles were mixed valence and their spectral characteristics did not match those of any known Fe mixed valence mineral phases (Fig. 2b); likely because of the variability in the chemistry and extent of oxidation in natural colloids and structural amorphism. Similarly, the ΔeV versus intensity ratio values of purely Fe(II) phases did not agree with any of the plotted points for literature reported standard mineral phases (e.g. pyrite). Again, variability in the chemistry of bonded inorganic and organic ligands, the presence of structural impurities and the extent of oxidation were invoked to explain

this mismatch. One likely explanation for the prevalence and persistence of Fe(II) enriched phases at these sites is that they are being stabilised by organic-rich surface coatings.

### *Pacific Ocean samples*

Over sixty particles were analysed from various depths (30-1000 m) at the three sampling sites in the South Pacific Ocean (SI 1). The majority of these particles (~80%) had Fe(II) as the dominant oxidation state with mostly pure Fe(II) and a few Fe(II)-rich mixed valence phases identified (Fig. 2b). Given the proximity of the sampling locations to sites of active tectonism<sup>21</sup> (SI 1), a proportion of the reduced Fe flux could be from associated hydrothermal sources<sup>13,22,23</sup>.

Figure 2b shows that the spectral parameters of Fe(II)-rich particles sampled from the Pacific Ocean have the largest range in distribution ( $\Delta E_V$ : 1.5-2.8; intensity ratio: 1.0-5.4) and that data points did not cluster around any of the standard mineral phases reported in the literature. Particles analysed in this study ranged from as small as 60 nm and up to 2.3  $\mu\text{m}$ ; with the average particle size tending towards larger values (mean = 0.70  $\mu\text{m}$ , N = 50). The smallest sized particles were characterised by the smallest intensity ratio and  $\Delta E_V$  values and, as particle size increased, there was a slight positive and increasing trend with both of the spectral parameters (SI 4). Although the increase in intensity ratio with particle size (or thickness) can partially be explained by STXM saturation effects, the observed variation in  $\Delta E_V$  value is a definitive indication of chemical or structural differences between the smallest colloids and larger particles.

### *Lacustrine samples*

Of the two lacustrine settings investigated, only the Pine Barrens samples showed appreciable Fe(II) abundance when examined using the Fe L-edge XANES spectroscopy. Only three discrete Fe-rich particles, ranging in size between 500 nm and 1  $\mu\text{m}$ , were investigated in detail at this site and all had spectra indicative of Fe(II) (Fig. 2b). The spectral parameters for these Fe(II) particles did not precisely match any of the examined standard Fe mineral phases, however one of the particles had spectral features similar to that of Fe(II)PO<sub>4</sub>, whereas the other two had Fe coordination environments most similar to that of Fe in biotite (Fig. 2b).

For the freshwater lake, Lake La Plata, large sized samples could be collected because of the sediment trap system installed for sampling at different depths. Although these samples showed 2-5% Fe, the X-ray diffraction of these samples indicated only the presence of K-mica, kaolinite and quartz, suggesting that the Fe phases are either amorphous or nanocrystalline. The L-edge spectromicroscopy of particulate samples collected from the top and bottom parts of the water column showed only Fe(III).

Comparison of the spectral features of these natural ferric phases to those of standard Fe-oxide and –oxyhydroxides, showed that ~21% of these particles have  $\Delta E_V$  and intensity ratio values characteristic of the crystalline standards. The majority (two thirds) of these had spectral features typically of goethite ( $\alpha\text{FeOOH}$ ), a phase which has previously been shown to be a dominant Fe-mineral phase in lacustrine waters<sup>24</sup>.

In contrast to the Fe L-edge, the bulk Fe-XANES spectra of particulates at the Fe K-absorption edge indicated the presence of a significant fraction of Fe(II). Linear combination fitting of bulk Fe K-edge XANES spectra indicated that there was appreciable (16-38%) Fe(II) associated with the lacustrine Fe particulates, irrespective of sampling season and sampling depth (SI 3). This disagreement in the L-edge and K-edge data comes from the sizes of particulates probed; K-edge XANES is carried out at ~7000 eV where the X-ray beams can penetrate deeper into the sample. Since the particulate concentration is very high for Lake La Plata samples, the particulates form large aggregates (several microns diameter) which can be probed for their bulk chemistry by the K-edge XANES, whereas the L-edge XANES could be used to focus on the smaller nanometer-sized fraction away from the large aggregates.

### **Speciation of colloidal organic carbon and its association with Fe phases**

Carbon K-edge XANES spectra were used to identify the predominant functional groups of organic molecules associated with Fe in marine and lacustrine particulates (Figs. 1, 3), and were further used in comparison against C XANES spectra from organics not associated with Fe (Fig. 3b). All C spectral features were classified into the following broad classes because of their common occurrence: (1) unsaturated carbon, including both carbon double and triple bonds, is associated with C  $1s \rightarrow \pi^*$  transitions at approximately 285 eV; (2) aryl- and vinyl-keto functional groups at approximately 286.0-286.4 eV; (3) aliphatic carbon, heterocycles and aldehydes at 286.5- 287.4 eV; (4) amide, ketone, and carboxylate at 287.5-288.8 eV; and (5) alcohol, carboxamide, and carbonate at 289.5-290.5 eV (SI 5). Although ideal for mapping purposes, the STXM resolution of ~10 nm limits the specificity of the chemical probe for detecting a specific organic ligand or functional group *binding* Fe, and the C K-edge spectra derived from each pixel are averaged spectra of many organic molecules present in that region. Hence the specific organic moieties *associated* with the Fe(II) and Fe(III) phases were investigated.

Marine data represent thirty Fe(II) particles, five Fe mixed-valence particles and two Fe(III) particles, whereas lacustrine data are averaged from four Fe(III) particles and three Fe(II) particles. In each instance, the corresponding number of analyses was conducted on Fe-poor regions of the  $\text{SiN}_3$  sample window to generate the data shown in Figure 3b. Irrespective of the particle chemical speciation or the aquatic sampling regime, all of the Fe particles evaluated showed significant association with

organic carbon of heterogeneous functional group chemistry. Relative to Fe-poor regions, Fe-rich regions typically show greater variety and prevalence in organic functional group chemistry. Despite a host of chemical and biological differences between the two sampling regimes, marine and lacustrine Fe(II) particles show similar trends in their association with organic carbon functional groups. However, Fe(III) particulates collected from lacustrine settings have an absence of aryl- and vinyl-keto functional groups and are associated with less alcohol and carboxamide moieties than their marine Fe(III) counterparts. These alcohol and carboxamide moieties are also much more strongly associated with particulates containing Fe(II) (including mixed valence phases), relative to Fe(III) particulates. Since carboxamide related spectral features are common in microbial mats and biofilms, the presence of these spectral features in samples could imply regions of high microbial activity. This is supported by the N K-edge data for Fe(II) particulates which exhibit features between 400.8 and 401.8 eV (SI 5), suggesting the presence of amide and substituted N-heterocycles which are typically linked to biological activity. Alternative explanations for the preferential association of some organic functional groups (e.g. carboxamide) for Fe(II) are that these functional groups have a higher binding affinity to Fe(II) or that they play a role in stabilizing Fe in its reduced valence state<sup>13</sup>.

Our X-ray spectroscopy and microscopy analyses have confirmed the ubiquity of Fe(II) colloids in a range of oxic aquatic environments, where the kinetics for oxidation to Fe(III) are known to be rapid<sup>25,26</sup>. Our observations of Fe(II) colloidal associations with organic carbon provide a plausible explanation for Fe(II) stability in oxygenated waters. The observed associations are also likely to have an impact on our understanding of Fe behaviour in the natural systems, where Fe mineral phases are known to play important roles in biological growth<sup>30</sup>, contaminant redox transformation processes<sup>5,27-29</sup> and in nutrient and contaminant transport fluxes<sup>1,2,4</sup>.

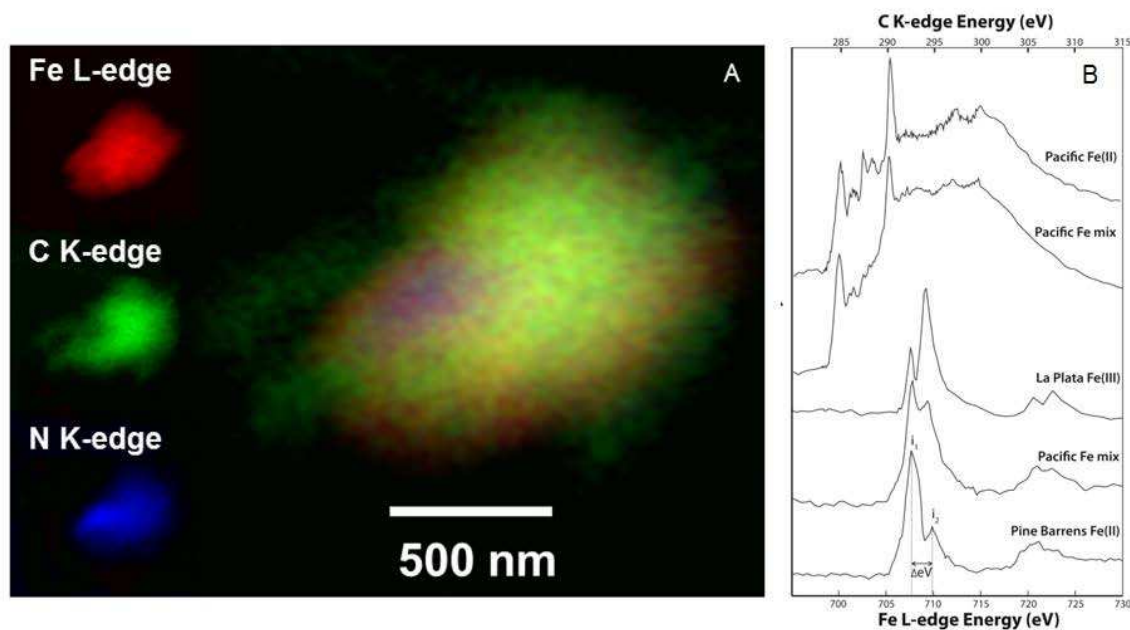
## **ACKNOWLEDGEMENTS**

This research is supported by grants from NRF, South Africa (Blue Skies Program), Stellenbosch University VR(R) fund, NSF (chemical sciences), US-DOE (BES & SBR), and Princeton in Africa program. Fieldwork was partly funded by the Australia Marine National Facility, GEOTRACES, CSIR (SOCCO) and IRGS grant L0018934 from the University of Tasmania. The authors would like to thank the support staff at the Advanced Light Source for helping with data collection and sample preparation. The authors would further like to acknowledge J. Compton and M. Lohan for their useful comments during review. This is AEON publication no. 120.

## **ASSOCIATED CONTENT**

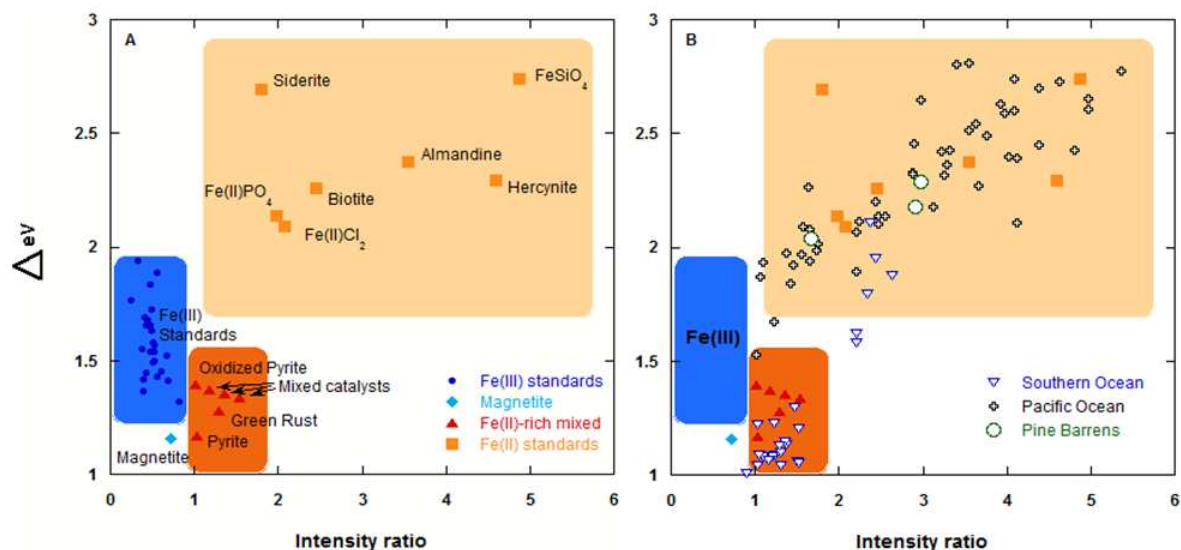
**Supporting Information:** Sample collection (SI 1); Soft X-ray spectromicroscopy studies (SI 2); Fe K-edge XANES analyses (SI 3); Spectral variations with particle size (SI 4); C K-edge and N K-edge spectral peak data (SI 5). All supporting information is available free of charge via the Internet at <http://pubs.acs.org>.

## FIGURES



218

**Figure 1a:** Association of Fe, C and N for a small marine particle. Although soft X-ray STXM provides high resolution imaging (~12 nm), particles cannot be distinguished from particle aggregates and the former terminology is used throughout the text. **1b:** Representative C K-edge (top two spectra) and Fe L-edge (bottom three spectra) XANES spectra for particles collected from a variety of aquatic sampling sites and with differing Fe chemistries. The characteristic L<sub>3</sub> peak splitting is parameterized according to its ΔeV value (difference in energy between the high energy and the low energy peaks) and its intensity ratio value (peak intensity quotient i<sub>1</sub>/i<sub>2</sub>).



58 |

**Figure 2a:** Intensity ratio versus  $\Delta eV$  characterization plot for Fe-rich standard phases collected from the literature (adapted from von der Heyden and co-workers<sup>15</sup>). Iron phases with different valences can clearly be distinguished by their unique fields on the plot. **2b:** Distribution of natural Fe(II) and Fe(II)-rich mixed-valence phases collected from four different aquatic sampling sites, plotted on the intensity ratio versus  $\Delta eV$  diagram.

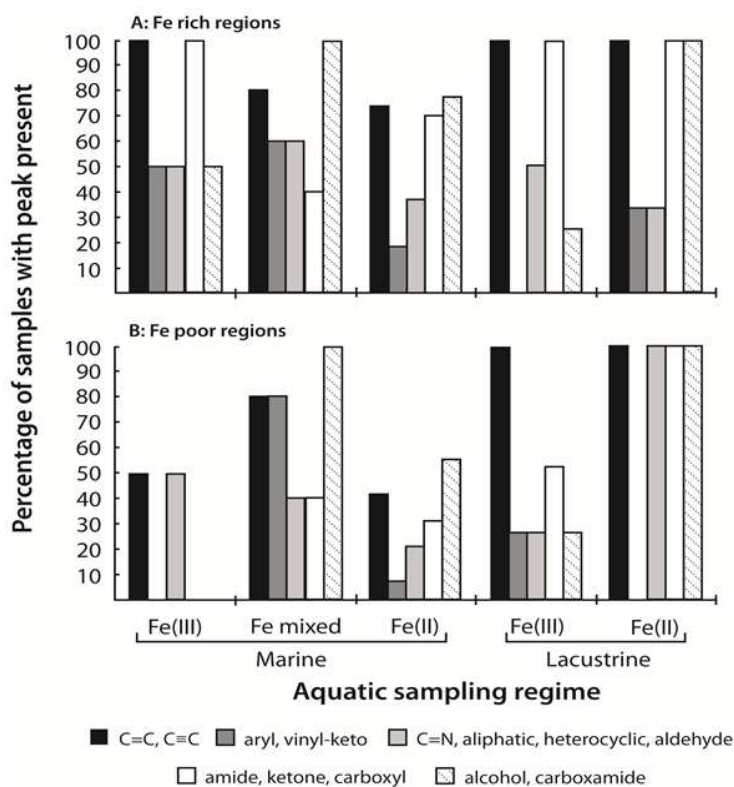


**Figure 3a:** Frequency of each set of organic functional groups as found in association with Fe-rich particulates of varying chemistry and sampling location. **3b:** Corresponding analyses of organic functional group frequency for Fe-poor regions of each particle or sample window. Additional data is presented in SI 5.

## REFERENCES

- (1) Hochella, M. F., Moore, J. N., Putnis, C. V., Putnis, A., Kasama, T., Eberl, D. D. Direct observation of heavy metal-mineral association from the Clark Fork River Superfund Complex: Implications for metal transport and bioavailability. *Geochim. Cosmochim. Acta* **2005**, *69*, 1651-1663.
- (2) Hassellöv, M.; von der Kammer, F. Iron oxides as geochemical nanovectors for metal transport in soil-river systems. *Elements Mag.* **2009**, *4*, 401-406.
- (3) Elsner, M.; Schwarzenbach, R. P.; Haderlein, S. B. Reactivity of Fe(II)-bearing minerals toward reductive transformation of organic contaminants. *Environ. Sci. Technol.* **2004**, *38*, 799-807.
- (4) Waychunas, G. A.; Kim, C. S.; Banfield, J. F. Nanoparticulate iron oxide minerals in soils and sediments: unique properties and contaminant scavenging mechanisms. *J. Nanopart. Res.* **2005**, *7*, 409-433.
- (5) Borch, T.; Kretzschmar, R.; Kappler, A.; Cappellen, P. V.; Ginder-Vogel, M.; Voegelin, A.; Campbell, K. Biogeochemical redox processes and their impact on contaminant dynamics. *Environ. Sci. Technol.* **2009**, *44*, 15-23.
- (6) Lanzirrotte, A. Application of hard X-ray microprobe methods to clay rich materials. In G. Waychunas (ed.), *CMS Workshop Lecture Series v. 18: Advanced Applications of Synchrotron Radiation in Clay Science*. **In press**.
- (7) Myneni, S. C. B. X-ray microscopy and spectromicroscopy. In G. Waychunas (ed.), *CMS Workshop Lecture Series v. 18: Advanced Applications of Synchrotron Radiation in Clay Science*. **In press**.
- (8) Bluhm, H.; Andersson, K.; Araki, T.; Benzerara, K.; Brown, G. E.; Dynes, J. J.; Ghosal, S.; Gilles, M. K.; Hansen, H.-Ch.; Hemminger, J. C.; Hitchcock, A. P.; Ketteler, G.; Kilcoyne, A. L. D.; Kneedler, E.; Lawrence, J. R.; Leppard, G. G.; Majzlam, J.; Mun, B. S.; Myneni, S. C. B.; Nilsson, A.; Ogasawara, H.; Ogletree, H. F.; Pecher, K.; Salmeron, M.; Shuh, D. K.; Tonner, B.; Tylliszczak, T.; Warwick, T.; Yoon, T. H. Soft X-ray microscopy and spectroscopy at the molecular environmental science beamline at the Advanced Light Source. *J. Electron Spectrosc.* **2006**, *150*, 86-104.
- (9) Dynes, J. J.; Tylliszczak, T.; Araki, T.; Lawrence, J. R.; Swerhone, G. D. W.; Leppard, G. G.; Hitchcock, A. P. Speciation and quantitative mapping of metal species in microbial biofilms using scanning transmission X-ray microscopy. *Environ. Sci. Technol.* **2006**, *40*, 1556-1565.
- (10) Chan, C. S.; Fakra, S. C.; Edwards, D. C.; Emerson, D.; Banfield, J. F. Iron oxyhydroxide mineralization on microbial extracellular polysaccharides. *Geochim. Cosmochim. Acta.* **2009**, *73*, 3807-3818.
- (11) Miot, J.; Benzerara, K.; Morin, G.; Kappler, A.; Bernard, S.; Obst, M.; Férard, C.; Skouri-Panet, F.; Guigner, J.-M.; Posth, N.; Galvez, M.; Brown Jr. G. E.; Guyot, F. Iron biomineralization by anaerobic neutrophilic iron-oxidizing bacteria. *Geochim. Cosmochim. Acta* **2009**, *73*, 696-711.
- (12) Schroth, A. W.; Crusius, J.; Sholkovitz, E. R.; Bostick, B. C. Iron solubility driven by speciation in dust sources to the ocean. *Nat. Geosci.* **2009**, *2*, 337-340.
- (13) Toner, B. M.; Fakra, S. C.; Manganini, S. J.; Santelli, C. M.; Marcus, M. A.; Moffett, J. W.; Rouxel, O.; German, C. R.; Edwards, K. J. Preservation of iron(II) by carbon-rich matrices in a hydrothermal plume. *Nat. Geosci.* **2009**, *2*, 197-201.
- (14) Lam, P. J.; Ohnemus, D. C.; Marcus, M. A. The speciation of marine particulate iron adjacent to active and passive continental margins. *Geochim. Cosmochim. Acta* **2012**, *80*, 108-124.

- (15) Von der Heyden, B. P.; Roychoudhury, A. N.; Mtshali, T. N.; Tylliszczak, T.; Myneni, S. C. B. Chemically and geographically distinct solid-phase iron pools in the Southern Ocean. *Science* **2012**, *338*, 1199-1201.
- (16) Lam, P. J.; Bishop, J. K. B. The continental margin is a key source of iron to the HNLC North Pacific Ocean. *Geophys. Res. Lett.* **2008**, *35*, L07608.
- (17) Hocking, R. K., De Beer George, S., Raymond, K. N., Hodgson, K. O., Hedman, B., Solomon, E. I. Fe L-edge X-ray absorption spectroscopy determination of differential orbital covalency of siderophore model compounds: electronic structure contributions to high stability constants. *J. Am. Chem. Soc.* **2010**, *132*, 4006-4015.
- (18) Peak, D; Regier, T. Direct observation of tetrahedrally co-ordinated Fe(III) in ferrihydrite. *Environ. Sci. Technol.* **2012**, *46*, 3163-3168.
- (19) Cutter, G.; Andersson, P.; Codispoti, L.; Croot, P.; Francois, R.; Lohan, M.; Obata, H.; van der Loeff, M.R. Sampling and sample-handling protocol for GEOTRACES cruises. **2010**, 39-51.
- (20) Monteiro, P. M. S.; van der Plas, A. K. Low Oxygen Water (LOW) variability in the Benguela system: key processes and forcing scales relevant to forecasting. In: Shannon V, Hempel G, Malanotte-Rizzoli P, Moloney C, Woods J (eds) Benguela: predicting a large marine ecosystem. Large marine ecosystems **2006**, *14*, Elsevier, Amsterdam, 91–109.
- (21) Mortimer, N.; Herzer, R. H.; Gans, P. B.; Parkinson, D. L.; Seward, D. Basement geology from the Three Kings Ridge to West Norfolk Ridge, southwest Pacific Ocean: evidence from petrology, geochemistry and isotopic dating of dredge samples. *Mar. Geol.* **1998**, *148*, 135-162.
- (22) Tagliabue, A.; Bopp, L.; Dutay, J.-C.; Bowie, A. R.; Chever, F.; Jean-Baptiste, P.; Bucciarelli, E.; Lannuzel, D.; Remenyi, T.; Sarthou, G.; Aumont, O.; Gehlen, M.; Jeandel, C. Hydrothermal contribution to the dissolved iron inventory. *Nat. Geosci.* **2010**, *3*, 252-256.
- (23) Bennett, S. A.; Achterberg, E. P.; Connelly, D. P.; Statham, P. J.; Fones, G. R.; German, C. R. The distribution and stabilization of dissolved Fe in deep-sea hydrothermal plumes. *Earth Planet. Sc. Lett.* **2008**, *270*, 157-167.
- (24) Van der Zee, C.; Roberts, D. R.; Rancourt, D. G.; Slomp, C. P. Nanogoethite is the dominant reactive oxyhydroxide phase in lake and marine sediments. *Geology* **2003**, *31*, 993-996.
- (25) Millero, F. J.; S. Sotolongo, S.; Izaguirre, M. The oxidation-kinetics of Fe(II) in seawater. *Geochim. Cosmochim. Acta* **1987**, *51*, 793-801.
- (26) Rose, A. L.; Waite T. D. Kinetic model for Fe(II) oxidation in seawater in the absence and presence of natural organic matter. *Environ. Sci. Technol.* **2002**, *36*, 433–444.
- (27) Williams, A. G. B.; Scherer, M. M. Kinetics of Cr(VI) reduction by carbonate green rust. *Environ. Sci. Technol.* **2001**, *35*, 3488-3494.
- (28) O'Loughlin, E. J.; Kelly, S. D.; Csencsits, R.; Cook, R. E.; Kemner, K. M. Reduction of uranium(VI) by mixed iron(II)/iron(III) hydroxide (green rust): Formation of UO<sub>2</sub> nanoparticles. *Environ. Sci. Technol.* **2003**, *37*, 721-727.
- (29) O'Loughlin, E. J.; Kelly, S. D.; Kemner, K. M.; Csencsits, R.; Cook, R. E. Reduction of Ag<sup>I</sup>, Au<sup>III</sup>, Cu<sup>II</sup>, and Hg<sup>II</sup> by Fe<sup>II</sup>/Fe<sup>III</sup> hydroxysulfate green rust. *Chemosphere* **2003**, *53*, 437-446
- (30) Chen, M.; Dei, R. C. H.; Wang, W.; Guo, L. Marine diatom uptake of iron bound with natural colloids of different origins. *Mar. Chem.* **2003**, *81*, 177-189.
- (31) Boyd, P. W.; Ellwood, M. J. The biogeochemical cycle of iron in the ocean. *Nat. Geosci.* **2010**, *3*, 675-682.

(32) Kneeder, E. M.; Rothe, J.; Weissmahr, K. W.; Pecher, K.; Tonner, B. P. Identification of green rust in environmental compounds using XANES of Fe-L<sub>II,III</sub> edges. In *Advanced Light Source Annual Compendium of Abstracts*, Lawrence Berkeley Publications **1997**.